Chickpea peel waste as sustainable precursor for synthesis of fluorescent carbon nanotubes for bioimaging application

Article *in* Carbon Letters · May 2020

DOI: 10.1007/s42823-020-00156-8

CITATIONS
13

READS
171

6 authors, including:

Vikram Singh
Central Institute of Mining and Fuel Research
17 PUBLICATIONS **350** CITATIONS
SEE PROFILE

Shovon Chatterjee
Indian Institute of Technology Kanpur
11 PUBLICATIONS **52** CITATIONS
SEE PROFILE

Mahendra Palecha
Indian Institute of Technology Kanpur
1 PUBLICATION **13** CITATIONS
SEE PROFILE

Pratik Sen
Indian Institute of Technology Kanpur
139 PUBLICATIONS **2,358** CITATIONS
SEE PROFILE

Chickpea peel waste as sustainable precursor for synthesis of fluorescent carbon nanotubes for bioimaging application

Vikram Singh, Shovon Chatterjee, Mahendra Palecha, Pratik Sen, Bushra Ateeq & Vivek Verma

Carbon Letters

ISSN 1976-4251

Carbon Lett.
DOI 10.1007/s42823-020-00156-8

Springer

Carbon Letters
https://doi.org/10.1007/s42823-020-00156-8

Online ISSN 2233-4998
Print ISSN 1976-4251

ORIGINAL ARTICLE

Chickpea peel waste as sustainable precursor for synthesis of fluorescent carbon nanotubes for bioimaging application

Vikram Singh[1] · Shovon Chatterjee[2] · Mahendra Palecha[3] · Pratik Sen[2] · Bushra Ateeq[3] · Vivek Verma[1,4]

Received: 20 March 2020 / Revised: 17 May 2020 / Accepted: 19 May 2020

Abstract

In this study, we report a controlled one-pot green synthesis of multiwalled carbon nanotubes (MWCNTs) via pyrolysis of sustainable agriculture waste (chickpea peel) at 400 °C in aqueous medium. These MWCNTs demonstrated 7.0 nm diameter, 0.28 nm graphitic spacing with carbonyl, hydroxyl, and carboxylic acid functionality. The D band (presence of sp^3 defects) and G band (E_{2g} mode of graphite) at 1350 cm^{-1} and 1580 cm^{-1} originated in Raman spectrum, respectively. The prepared MWCNTs showed blue fluorescence with 10% fluorescence quantum yield in aqueous medium. The MWCNTs showed triple exponential decay characteristics with an average fluorescence lifetime of 4.7 ns. The synthesized MWCNTs revealed a consistent fluorescence in the cytoplasm of 22RV1 human prostate carcinoma cell line without exerting any sign of cytotoxicity. The MWCNTs also exhibited remarkable cytocompatibility in human immortalized prostate epithelial RWPE1 cells.

Graphic abstract

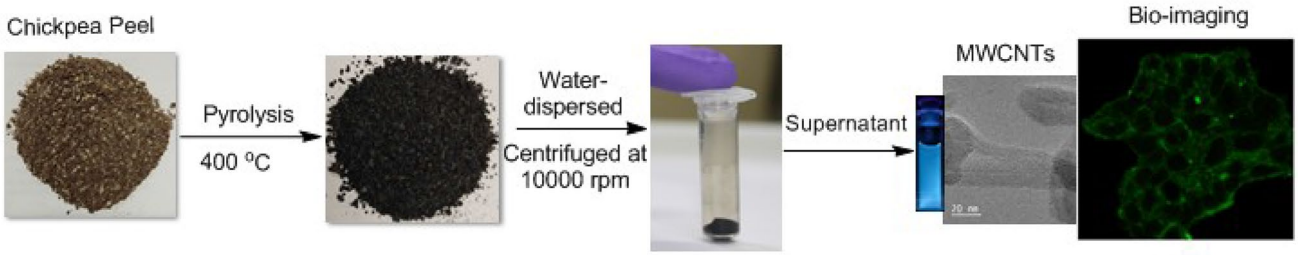

Keywords Chickpea peel waste · Agriculture waste · Pyrolysis · Fluorescent MWCNTs · Cancer cell imaging

1 Introduction

Multiwall carbon nanotubes (MWCNTs) are emerging as a new class of environmentally friendly fluorescent carbon-based nanomaterials [1, 2]. They have potential to replace conventional organic fluorescent dyes and metal-based quantum dots because of broad absorption spectrum, low background, high signal-to-noise ratio, label-free detection, real-time monitoring, high sensitivity, their simple preparation, tunability in emission, photochemical stability, high biocompatible, and easily dispersibility in aqueous medium [3, 4]. Based on tuneable fluorescence (UV–visible to near IR) properties of MWCNTs, CNTs have been extensively explored for electrochemical [5], theranostics [6], tissue engineering [7], composite material [8], and drug delivery

Electronic supplementary material The online version of this article (https://doi.org/10.1007/s42823-020-00156-8) contains supplementary material, which is available to authorized users.

✉ Vikram Singh
vikramsg@iitk.ac.in; vikku.010@gmail.com

✉ Vivek Verma
vverma@iitk.ac.in

[1] Department of Materials Science and Engineering, Indian Institute of Technology Kanpur, Kanpur 208016, India

[2] Department of Chemistry, Indian Institute of Technology Kanpur, Kanpur 208016, India

[3] Department of Biological Sciences and Bioengineering, Indian Institute of Technology Kanpur, Kanpur 208016, India

[4] Centre for Environmental Science and Engineering, Indian Institute of Technology Kanpur, Kanpur 208016, India

Published online: 29 May 2020

and bioimaging [4, 9, 10] applications. Recent studies with carbon nanomaterials having longer emission wavelength displayed its importance in cell imaging, some of which used in organelle specific localisation. One such study on naphthalimide-derived carbon dots demonstrated its ability to detect endogenous formaldehyde in lysosomes via fluorescence imaging [11, 12]. In addition, their unique mechanical, electrical, and thermal properties make them attractive candidates for applications in the field of electronic, environment, chemical, and biomedical science [13–18]. Large quantities of MWCNTs may be produced from carbon rich materials using methods like arc discharge, laser ablation, chemical vapor deposition, and pyrolysis [19–24]. However, above-discussed methodologies are not advantageous for establishing a green synthetic method and raise environmental issues. Recently, fluorescent carbon-based nanomaterials are synthesized using agriculture waste materials paving way as greener, cost-effective, and environmentally benign methods [25, 26]. In recent years, CNTs have been widely studied as in vitro and in vivo imaging agents. For examples, Hasan et al. introduce a novel method for in vivo imaging of the biodistribution of single-wall carbon nanotubes (SWCNTs) labeled with recombinant thermo-stable Luciola cruciate luciferase (LcL). They found for the first time that LcL chemically bound to SWCNTs was a powerful tool for CNTs' in vivo imaging applications [27]. Cui and his co-workers demonstrated silica-coated gold nanorods on the surface of MWCNTs for targeted photoacoustic imaging of gastric cancer cells in vivo [28]. The synthesized silica-coated gold nanorods/MWCNT showed low cellular toxicity and good water solubility which could target gastric cancer cells in vivo as well as in the nude model. A sustainable and cost-effective process for large-scale production of MWCNTs is highly desirable due to above applications. One of the challenges is an abundant, cost-effective source of carbon for CNT production. Therefore, we looked at agriculture waste, such as chickpea peel that is a good source of dietary fiber with, almost 40% of their peels containing fiber in the form of celluloses, hemicelluloses, and pectins [29]. In this article, we report synthesis of water dispersible MWCNTs from pyrolysis of chickpea peel. The morphological characterization, photophysical studies, bioimaging application, and in vitro cytotoxicity of the MWCNTs discussed.

2 Experimental details

2.1 Materials

The ripe *Cicer arietinum* (chickpea) was obtained from local market of Kanpur, India. The peel was removed from ripe chickpea for further use. Spectroscopic grade solvents were purchased from Sigma-Aldrich and used without further purification.

2.2 Instrumentation

UV–Vis absorption and emission spectra were recorded on a commercial spectrophotometer (UV-2450, Schimadzu, Japan) and fluorimeter (Fluoromax-4, Jobin–Yvon, USA), respectively. Fluorescence lifetime was measured using a commercial time-correlated single-photon counting (TCSPC) setup (Life Spec II, Edinburgh Instruments, UK). A 375.8 nm diode laser (EPL-375, Edinburgh Instruments, UK) was used as the excitation source. The full width at the half maxima of the instrument response function (IRF) was about 120 ps. The fluorescence transient was fitted with sum of two exponentials along with the deconvolution with the IRF to obtain the lifetime. The length and diameter of CNTs were measured using FEI Titan G2 300 kV high-resolution transmission electron microscope (HR-TEM). The surface functionality characterization was carried out by X-ray photoelectron spectroscopy (XPS) using PHI 5000 Versaprobe II, FEI. Zeta-potential measurement was done in aqueous solution with Malvern Zetasizer Nano ZS 90 to measure the surface charge on MWCNTs. The confocal imaging was done using LSM780NLO laser scanning microscope (Carl Zeiss Germany). Excitation filter for CNT was set at 488 nm and emission filter set in the range of 500–550 nm with 60× objective. Fourier transform infrared spectra (Perkin Elmer Spectrum version 10.03.06) were recorded using the KBr pellet method.

2.3 Preparation of multiwall carbon nanotubes from chickpea peel

The preparation of MWCNTs from chickpea peel was carried out by pyrolysis treatment as follows. The chickpea peel was grinded using domestic mixer grinder. The grinded chickpea peel (5.0 g) was kept for carbonization in the furnace for 4.0 h at 400 °C (3 °C/min) following which the furnace was allowed to cool to room temperature. Cellulose rich chickpea peel when heated at 400 °C in the furnace first decomposes into carbon, oxygen, and hydrogen species; hydrogen flies away. Oxygen helps to initiate the CNT precipitation at the nucleation stage, forming an embryonic cap from which subsequent MWCNT growth takes place. The obtained 1.0 g of pyrolyzed chickpea peel carbon was dispersed in distilled water and then sonicated for 10 min using probe sonicator (Vibra-CellTM Ultrasonic Processor, VCX750). Furthermore, the colloidal solution was centrifuged at 11000 rpm for 15 min and supernatant solution was collected. The supernatant was treated with a dialysis bag (MWCO 1 kDa) for 24 h to remove unreacted small chemicals.

In general, the low-temperature pyrolysis (400–800 °C) yields MWCNTs, which indicates that SWCNTs have a higher energy formation. That is why, MWCNTs are easier to grow without catalyst from most of the agriculture waste materials [30].

Finally, the purified MWCNTs having 4.0 mg/mL concentration were obtained in double-distilled water (DDW) and stored at 4 °C. In this green, economical, and simple approach, no carrier gas supplementary catalyst and substrate were used. The MWCNTs were freely dispersed in aqueous medium (Scheme 1).

2.4 Sample preparation for in vitro cell imaging

Prostate cancer 22RV1 cells were cultured on a glass cover slip at a density of 4×10^4 cells per well in a 4-well dish. The cells were supplemented with 10% fetal bovine serum in RPMI-1640 medium-containing 1% penicillin streptomycin, and incubated for 24 h at 37 °C under humidified 5% CO_2 atmosphere. The cells were treated with MWCNTs samples at 250 µg/mL for 24 h. The cells grown on the cover slip were washed thrice with 1 × phosphate-buffered saline (PBS) and fixed in 4% para formaldehyde for 20 min, and stained with 4′,6-diamidino-2-phenylindole (DAPI) after washing again with 1 × PBS twice, and after rinsing it with 1 × PBS, it was mounted on the glass slide using Vectashield mounting medium (Vector Labs). The images were captured on confocal microscope system (Zeiss LSM780NLO).

2.5 Cytotoxicity assay

In vitro cytotoxicity assay was performed using different concentrations of MWCNTs using Resazurin dye-based fluorescence measurement assay. Stock solutions of MWCNT samples were prepared at 4.0 mg/mL and dilutions were prepared from 100 to 0.1 µg/mL in cell culture medium. Both 22RV1 and RWPE1 cells were seeded at the density of 3×10^3 cells/well in 96-well cell culture plate. The cells were incubated in 5% CO_2 for 24 h at 37 °C in humidified conditions. The cells were next treated with different working concentrations of MWCNTs and incubated for another 24 h, while DI water was used as a control. After this, the medium in each well was replaced with 100 µL fresh medium-containing 8 µL of 0.25 mg/mL Resazurin and incubated for another 4 h. At last, the fluorescence was measured at the excitation–emission at 530–590 nm wavelength using Biotek Synergy H_4 hybrid microplate reader.

3 Characterization of chickpea peel-derived MWCNTs

3.1 Morphological characterization

The structural characteristics (morphology, length, and diameter) of MWCNTs synthesized from pyrolysis of chickpea peel at 400 °C were examined by high-resolution transmission electron microscope (HR-TEM). The HR-TEM images of pyrolyzed chickpea peel demonstrated MWCNTs' formation, as shown in Fig. 1a, b. The average length and diameter of synthesized CNTs was found to be 114.0 and 7.0 nm, respectively (Fig. S1 in Electronic Supplementary Information). The multiwall nature MWCNTs with approximately 20 layers of concentric graphene layers stacked together were observed in high-resolution TEM (HR-TEM). The HR-TEM image of MWCNTs indicated that the lattice spacing was 0.28 nm (Fig. 1b), which matched well with the facet of graphite [31]. The as-synthesized MWCNTs exhibit sp^2 graphitic properties similar to carbon quantum dots [32].

X-ray photoelectron spectroscopy (XPS) and FTIR technique were used to determine the functionalities at surface of MWCNTs. Two peaks at 281.4 and 532.0 eV attributed to C1s and O1s, respectively, in the full XPS spectrum of MWCNTs (Fig. 2a), which suggested chief composition of MWCNTs as C and O. The binding energy values of functional groups were obtained from high-resolution spectrum (full scan) for C1s and O1s. The deconvoluted C1s peak, corresponding to C–H/C–O at 285.4 eV, C–OH/C–O–C at 287.5 eV, and COOH at 289.3 eV (Fig. 2b) and one, corresponding to C–O at 532 eV (Fig. S2 in Electronic Supplementary Information) were observed. Signatures of functional groups such as 3405 cm^{-1} for stretching vibrations of

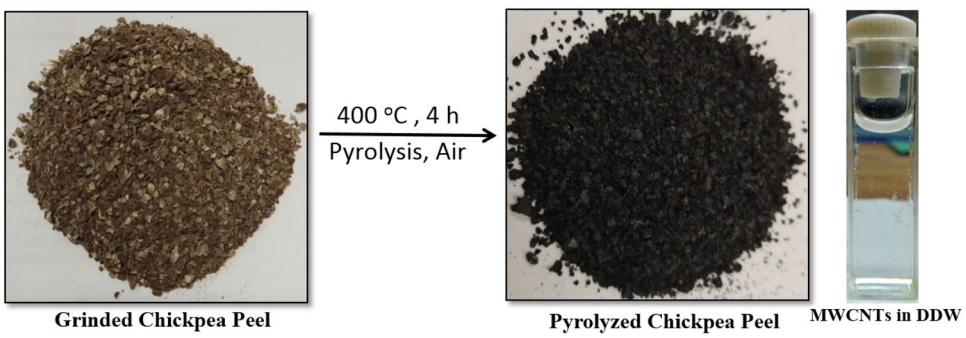

Scheme 1 Schematic representation for one-step synthesis of MWCNTs from pyrolyzed chickpea peel

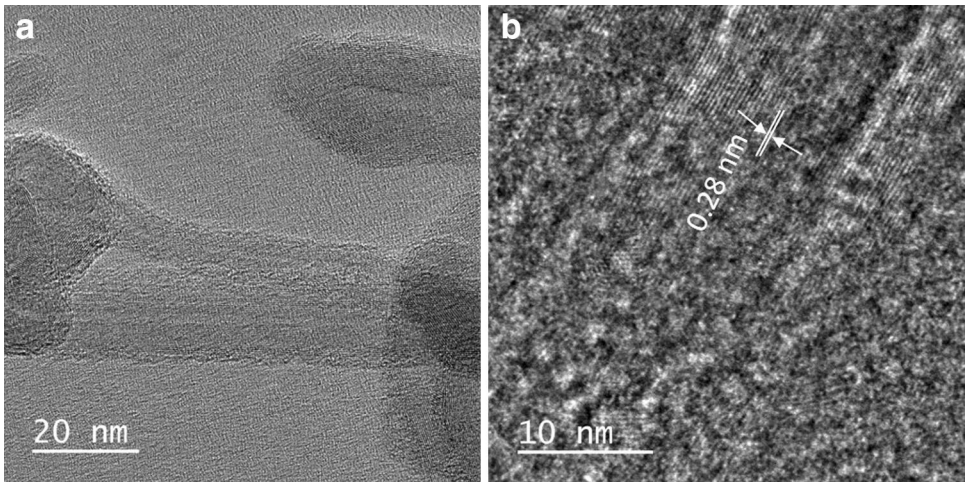

Fig. 1 **a** HR-TEM micrographs of MWCNTs obtained from pyrolysis of chickpea peel **b** with lattice spacing 0.28 nm; [MWCNTs] = 0.4 mg/mL MWCNTs

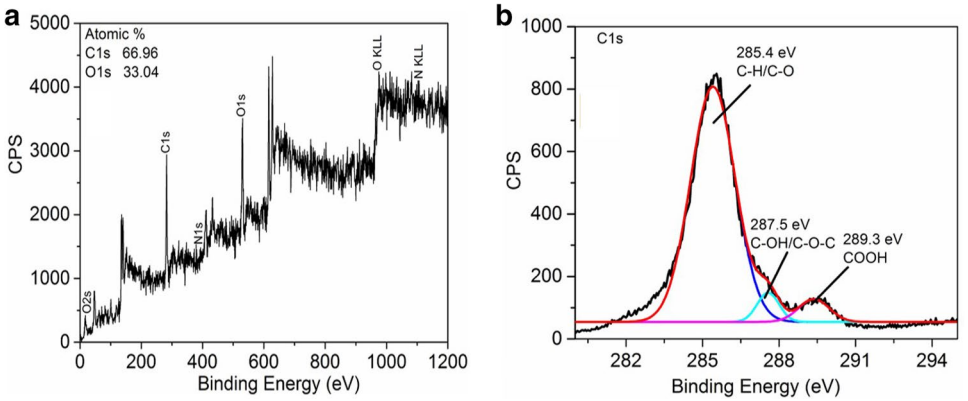

Fig. 2 Full-scan XPS analysis: **a** high-resolution XPS spectra and **b** C1s region of MWCNTs obtained from pyrolysis of chickpea peel

C–OH, 1552 cm^{-1} for C=C-stretching vibration, 1392 cm^{-1} C–C and 1240 cm^{-1} for C–O vibrations, etc., were observed in FTIR spectra (Fig. S3 in Electronic Supplementary Information). Both XPS and FTIR spectra indicated that MWCNTs were functionalized with carbonyl, hydroxyl and carboxylic acid groups. The zeta potential (ζ) of chickpea peel-derived MWCNTs was found to be − 29.7 mV at neutral pH, quite stable in the water. The negative value of zeta potential suggested acid functionalities on the surface of synthesized MWCNTs (Fig. S4 in Electronic Supplementary Information). The presence of these functional groups on the MWCNTs was reflected by excellent dispersion in water and cell membrane permeability.

Raman spectroscopy was employed to study the MWCNTs' structure and presence of disorder. The spectra corresponding to D band and G band at 1350 cm^{-1} and 1580 cm^{-1}, respectively, are observed in Fig. 3. The peak at 1580 cm^{-1} (G band) corresponded to an E_{2g} mode of graphite and related to the vibration of sp^2-bonded carbon atoms in a two-dimensional hexagonal lattice, such as in a graphite layer [32]. CNTs with concentric multiwalled layers of hexagonal carbon lattice display the same vibration [32]. The peak at 1350 cm^{-1} (D band) was related to the presence of

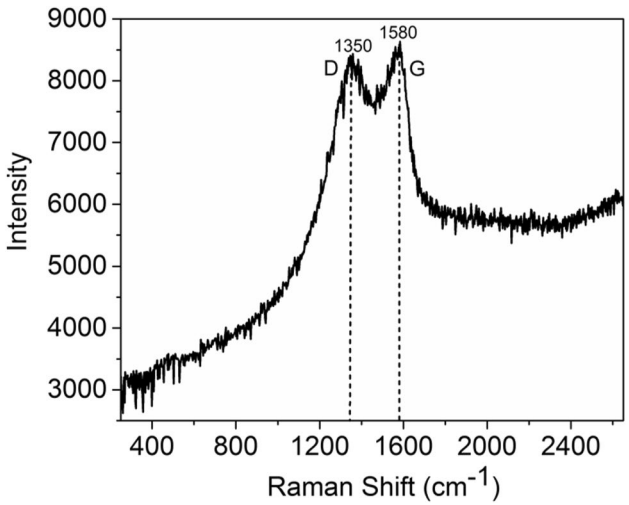

Fig. 3 Raman spectra of MWCNTs [Raman excitation @ 532 nm]

sp^3 defects. The presence of D and G band in Raman spectra indicated the formation of MWCNTs. The intensity of peak ratio between the G band and D band > 1 which indicates the formation of MWCNTs with higher purity.

3.2 Photophysical study

The detailed photophysical properties of fluorescent MWCNTs in aqueous medium were studied at room temperature (Fig. 4). Since the concentration of these MWCNTs cannot be calculated accurately, the absorbance of MWCNTs was kept in the range of 0.2–0.7 at excitation wavelength to avoid any inner filter effect. A clear transparent solution of 0.40 mg/mL MWCNTs showed strong absorption around 300–500 nm (Fig. 4a, black) and upon exciting at 365 nm emitted strong blue fluorescence (inset Fig. 4a) with maximum at 450 nm (Fig. 4a, blue). To measure the average fluorescence lifetime of blue-emitting MWCNTs, time-correlated single-photon counting (TCSPC) measurement was performed. The fluorescence transient at its maximum showed triple exponential decay characteristics (Fig. 4b) with an average fluorescence lifetime of 4.7 ns. The excitation wavelength dependence of the emission spectra is a common feature for carbon nano materials [33].

This actually manifests structural in homogeneity originated from different surface trap states. The presence of different kind of aggregate even in a very low concentration may also contribute to the excitation wavelength dependence of the emission spectra [34]. To explore the excitation-dependent emission property of the synthesized MWCNTs, we varied the excitation wavelength from 320 to 540 nm, with a 20 nm interval (Fig. S5a in Electronic Supplementary Information).

A prominent red shift in the fluorescence spectra was observed in this case (Fig. S5a, b in Electronic Supplementary Information). The fluorescence quantum yield of the blue-emitting MWCNTs in aqueous medium was found to be 10% (for $\lambda_{ex} = 350$ nm) taking quinine sulfate in 0.05 M H_2SO_4 as the standard.

4 Results and discussion

4.1 Bioimaging application

The utility of MWCNTs as non-toxic cell imaging probe was studied by incubating 22RV1 cells with MWCNTs' solution for 24 h in culture conditions as mentioned earlier. The fluorescent images were captured using confocal laser scanning microscope (Fig. 5).

The cell nuclei in blue indicated DAPI staining (Fig. 5a). The green fluorescence depicted the localization of MWCNTs in the cytoplasm and on the plasma membrane of the cells (Fig. 5). The morphology of 22RV1 cells remained unaltered upon treatment with MWCNTs.

In cytotoxicity assay, 22RV1 cells treated with different concentrations of MWCNTs (0.1–100 µg/mL) revealed no significant change in the cell viability, indicating biocompatibility properties of the MWCNTs (Fig. 6). We also tested higher concentration (1.0 mg/mL) of MWCNTs on these cells; interestingly, no change in cell membrane integrity or morphology was observed (data not shown), suggesting that the MWCNTs could be safely used in in vitro imaging of cells. Similar cytotoxicity experiment was performed with human immortalized prostate epithelial RWPE1 cells, wherein a marginal reduction (~ 18%) in the cell viability at 100 µg/mL of MWCNT concentration was noted. Collectively, our findings emphasized on the cytological compatibility and biocompatibility of the synthesized MWCNTs.

5 Conclusions

We demonstrate synthesis of highly fluorescent MWCNTs from the pyrolysis of chickpea peel using a green, one-step, low-cost method. The synthesized MWCNTs are of

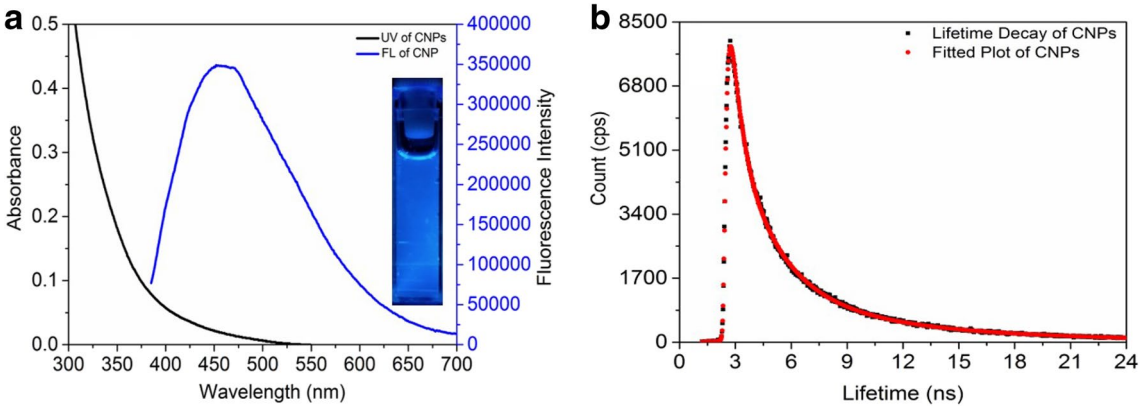

Fig. 4 **a** UV–visible absorption and emission spectra with blue fluorescent image (inset). **b** Time-resolved fluorescence decay in aqueous medium ($\lambda_{ex} = 375$ nm and $\lambda_{em} = 455$ nm) [MWCNTs] = 0.40 mg/mL

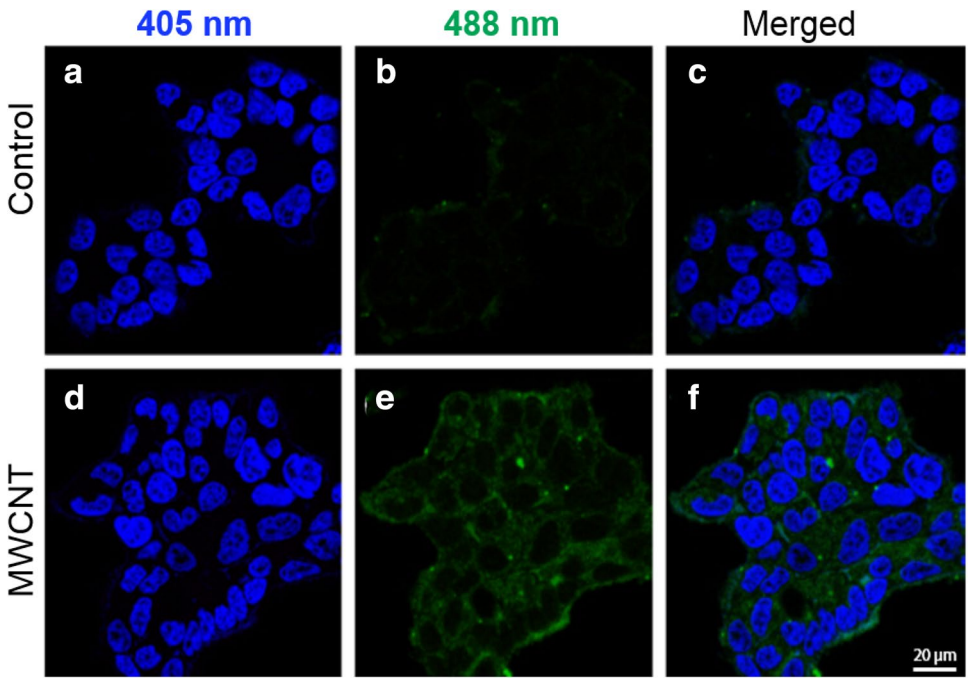

Fig. 5 Representative confocal microscopy images of 22RV1 cells treated with MWCNTs. **a** DAPI staining in control 22RV1 cells, **b** control 22RV1 cells without MWCNTs treatment, **c** merged image of control 22RV1 cells, **d** DAPI staining of 22RV1 cells treated with MWCNTs, **e** 22RV1 cells treated with MWCNTs (250 µg/mL) showing green fluorescence, and **f** merged image of MWCNTs treated 22RV1 cells. The 405 nm (λ_{em} = 425–475 nm) and 488 nm (λ_{em} = 500–550 nm) laser was used for confocal imaging

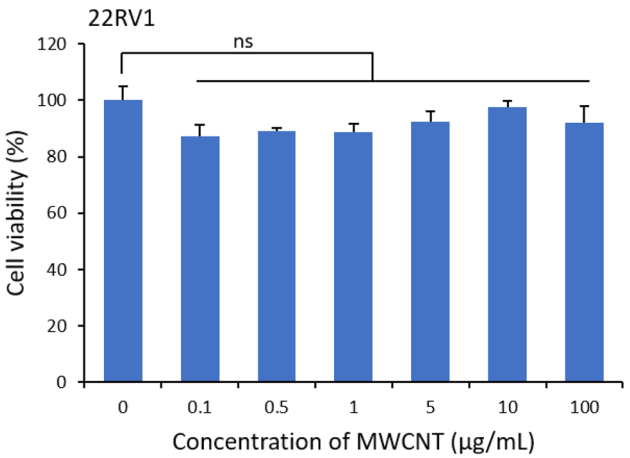

Fig. 6 Resazurin-based cytotoxicity assay using different concentrations of MWCNTs on prostate cancer 22RV1 cells after 24 h incubation at 37 °C (*ns* not significant)

nanometer-sized, exhibit good dispersibility in water, have strong and stable fluorescence. The MWCNTs exhibit excellent fluorescence property in the cytoplasm of 22RV1 cells, without showing any sign of cytotoxicity as well as excellent cytocompatibility in RWPE1 cells, making them potential candidates for bioimaging and biomedical applications.

Acknowledgements VS thank Department of Materials Science and Engineering, IIT Kanpur, India for fellowship (Institute Postdoctoral Fellowship) and funding (PDF 88). PS thanks Visvesvaraya PhD Programme of Ministry of Electronics and Information Technology (MeitY), Government of India for providing young faculty research fellowship. BA is thankful for the research funding from the Welcome Trust/DBT India Alliance (IA/I(S)/12/2/500635 to BA), Department of Biotechnology, Government of India (BT/PR8675/GET/119/1/2015) and the Science and Engineering Research Board (SERB) (EMR/2016/005273). We acknowledge advance imaging centre and advance centre for materials science, IIT Kanpur for HR-TEM and XPS study, respectively. This work was supported by Department of Science and Technology-Technology Systems Development Program (DST-TSDP) grant number DST/TSG/AMT/2015/329 awarded to VV.

Compliance with ethical standards

Conflict of interest The authors declare that they have no conflict of interest.

References

1. Jorio A, Dresselhaus G (2006) Advanced topics in the synthesis, structure. Springer Publishing House, Berlin, p 101
2. Tuaev X, Paraknowitsch JP, Illgen R, Thomas A, Strasser P (2012) Nitrogen-doped coatings on carbon nanotubes and their stabilizing effect on Pt nanoparticles. Phys Chem Chem Phys 14:6444–6447
3. Hatton RA, Miller AJ, Silva SRP (2008) Carbon nanotubes: a multi-functional material for organic optoelectronics. J Mater Chem 18:1183–1192
4. Wen J, Xu Y, Li H et al (2015) Recent applications of carbon nanomaterials in fluorescence biosensing and bioimaging. Chem Commun 51:11346–11358
5. Lota G, Fic K, Frackowiak E (2011) Carbon nanotubes and their composites in electrochemical applications. Energy Environ Sci 4:1592–1605
6. Liang C, Diao S, Wang C, Gong H, Liu T, Hong G, Shi X, Dai H, Liu Z (2014) Tumor metastasis inhibition by imaging-guided photothermal therapy with single-walled carbon nanotubes. Adv Mater 56:5646–5652

7. Harrison BS, Atala A (2007) Carbon nanotube applications for tissue engineering. Biomaterials 28:344–352
8. Hammel E, Tang X, Trampert M, Schmitt T, Mauthner K, Eder A, Pötschke P (2004) Carbon nanofibers for composite applications. Carbon 42:1153–1158
9. Iizumi Y, Yudasaka M, Kim J, Sakakita H, Takeuchi T, Okazaki T (2018) Oxygen-doped carbon nanotubes for near-infrared fluorescent labels and imaging probes. Sci Rep 8:6272
10. Boghossian AA, Zhang J, Barone PW, Reuel NF, Kim JH, Heller DA, Ahn JH, Hilmer AJ, Rwei A, Arkalgud JR, Zhang CT, Strano MS (2011) Near-infrared fluorescent sensors based on single-walled carbon nanotubes for life sciences applications. ChemSusChem 4:848–863
11. Liu J, Dong Y, Ma Y, Han Y, Ma S, Chen H, Chen X (2018) One-step synthesis of red/green dual-emissive carbon dots for ratiometric sensitive ONOO– probing and cell imaging. Nanoscale 10:13589–13598
12. Chen S, Jia Y, Zou GY, Yu YL, Wang JH (2019) A ratiometric fluorescent nanoprobe based on naphthalimide derivative-functionalized carbon dots for imaging lysosomal formaldehyde in HeLa cells. Nanoscale 11:6377–6383
13. Shi W, Plata DL (2018) Vertically aligned carbon nanotubes: production and applications for environmental sustainability. Green Chem 20:5245–5260
14. Arnold MS, Green AA, Hulvat JF, Stupp SI, Hersam MC (2006) Sorting carbon nanotubes by electronic structure using density differentiation. Nat Nanotechnol 1:60–65
15. Zhou J, Wang C, Qian Z, Chen C, Ma J, Du G, Chen J, Feng H (2012) Highly efficient fluorescent multi-walled carbon nanotubes functionalized with diamines and amides. J Mater Chem 22:11912–11914
16. Liu Z, Tabakman SM, Chen Z, Dai H (2009) Preparation of carbon nanotube bioconjugates for biomedical applications. Nat Protoc 4:1372–1381
17. Schnorr JM, Swager TM (2011) Emerging applications of carbon nanotubes. Chem Mater 23:646–657
18. Mohammadinejad R, Karimi S, Iravani S, Varma RS (2015) Plant-derived nanostructures: types and applications. Green Chem 18:20–52
19. Journet C, Maser WK, Bernier P, Loiseau A, Lamy de la Chapelle M, Lefrant S, Deniard P, Lee R, Fischer JE (1997) Large-scale production of single-walled carbon nanotubes by the electric-arc technique. Nature 388:756–758
20. Maser WK, Muñoz E, Benito AM, Martínez MT, De La Fuente GF, Maniette Y, Anglaret E, Sauvajol JL (1998) Production of high-density single-walled nanotube material by a simple laser-ablation method. Chem Phys Lett 292:587–593
21. Che G, Lakshmi BB, Martin CR, Fisher ER, Ruoff RS (1998) Chemical vapor deposition based synthesis of carbon nanotubes and nanofibers using a template method. Chem Mater 10:260–267
22. Cheng HM, Li F, Su G, Pan HY, He LL, Sun X, Dresselhaus MS (1998) Large-scale and low-cost synthesis of single-walled carbon nanotubes by the catalytic pyrolysis of hydrocarbons. Appl Phys Lett 72:3282–3284
23. Singh V, Rawat KS, Mishra S, Baghel T, Fatima S, John AA, Kalleti N, Singh D, Nazir A, Rath SK, Goel A (2018) Biocompatible fluorescent carbon quantum dots prepared from beetroot extract for in vivo live imaging in *C. elegans* and BALB/c mice. J Mater Chem B 6:3366–3371
24. Lara-Romero J, Ocampo-Macias T, Martínez-Suarez R, Rangel-Segura R, López-Tinoco J, Paraguay-Delgado F, Alonso-Nuñez G, Jiménez-Sandoval S, Chiñas-Castillo F (2017) Parametric study of the synthesis of carbon nanotubes by spray pyrolysis of a biorenewable feedstock: α-pinene, ACS sustain. Chem Eng 5:3890–3896
25. Zhuo C, Alves JO, Tenorio JAS, Levendis YA (2012) Synthesis of carbon nanomaterials through up-cycling agricultural and municipal solid wastes. Ind Eng Chem Res 51:2922–2930
26. Xu Y, Jia XH, Yin XB, He XW, Zhang YK (2014) Carbon quantum dot stabilized gadolinium nanoprobe prepared via a one-pot hydrothermal approach for magnetic resonance and fluorescence dual-modality bioimaging. Anal Chem 86:12122–12130
27. El-Sayed R, Eita M, Barrefelt Å et al (2013) Thermostable luciferase from Luciola cruciate for imaging of carbon nanotubes and carbon nanotubes carrying doxorubicin using in vivo imaging system. Nano Lett 13:1393–1398
28. Wang C, Bao C, Liang S et al (2014) RGD-conjugated silica-coated gold nanorods on the surface of carbon nanotubes for targeted photoacoustic imaging of gastric cancer. Nanoscale Res Lett 9:264
29. Niño-Medina G, Muy-Rangel D, De La Garza AL et al (2019) Dietary fiber from chickpea (*Cicer arietinum*) and soybean (glycine max) husk byproducts as baking additives: functional and nutritional properties. Molecules 24:991
30. Kumar M (2011) Carbon nanotube synthesis and growth mechanism. In: Carbon nanotubes—synthesis, characterization, applications. https://doi.org/10.5772/19331
31. Tuinstra F, Koenig JL (1970) Raman spectrum of graphite. J Chem Phys 53:1126. https://doi.org/10.1063/1.1674108
32. Eklund PC, Holden JM, Jishi RA (1995) Vibrational modes of carbon nanotubes; spectroscopy and theory. Carbon N Y 33:959–972
33. Lecroy GE, Messina F, Sciortino A, Bunker CE, Wang P, Fernando KAS, Sun YP (2017) Characteristic excitation wavelength dependence of fluorescence emissions in carbon "quantum" dots. J Phys Chem C 121:28180–28186
34. Sharma A, Gadly T, Gupta A, Ballal A, Ghosh SK, Kumbhakar M (2016) Origin of excitation dependent fluorescence in carbon nanodots. J Phys Chem Lett 7:3695–3702